2/2-22-83

UCRL--87735-Rev.1

DE83 004215

UCRL-87735 Rev. 1
PREPRINT

MASTER

THE (CHANGING) MFTF VACUUM ENVIRONMENT

David Margolies
Lawrence Valby

This paper was prepared for presentation at
National Vacuum Symposium
Baltimore, MD November 16, 1982

December 1982

Lawrence Livermore Laboratory

DISTRIBUTION OF THIS DOCUMENT [illegible]

THE (CHANGING) MFTF VACUUM ENVIRONMENT*

by

David Margolies and Lawrence Valby
Lawrence Livermore National Laboratory
University of California
Livermore, California 94550

ABSTRACT

The Mirror Fusion Test Facility (MFTF) vacuum vessel will be about 60m long and 10m in diameter at the widest point. The allowable operating densities range from 2 x 10^9 to 5 x 10^{10} particles per cc. The maximum leak rate of 10^{-6} tl/sec is dominated during operation by the deliberately injected cold gas of 250 tl/sec. This gas is pumped by over 1000 square meters of cryopanels, external sorbtion pumps and getters. The design and requirements have changed radically over the past several years, and they are still not in final form. The vacuum system design has also changed, but more slowly and less radically. This paper discusses the engineering effort necessary to meet these stringent and changing requirements. Much of the analysis of the internal systems has been carried out using a 3-D Monte Carlo computer code, which can estimate time dependent operational pressures. This code and its use will also be described.

---

*This work was performed under the auspices of the U. S. Department of Energy by Lawrence Livermore National Laboratory under Contract W-7405-Eng-48.

[illegible]

The Mirror Fusion Test Facility (MFTF) currently under construction at Lawrence Livermore National Laboratory (LLNL) is the latest of a series of mirror machines designed and built at LLNL, and one of the largest fusion machines to date, comparable in size and power to the TFTR at Princeton and the European JET. The proposal for MFTF was made in March 1976 and initial Department of Energy approval was given in 1977.

Since that time the machine has evolved. It has increased in size by a factor of 3, changing from a simple mirror to a tandem mirror machine. The vacuum system has evolved over that time as well, but its changes have been far less substantial. Additional capacity has been added as the machine grew, but no serious redesign has occurred. This paper will describe the high vacuum system of MFTF, trace its evolution and discuss the methods used in its design.

Section 2 describes the vacuum environment of the current design of MFTF along with a brief description of the vessel and its purpose. Section 3 will describe the evolution of the vacuum system. Section 4 describes the methods of analysis of the vacuum system. A three-dimensional Monte Carlo simulation program was extensively used to estimate the efficacy of designs and compare different approaches. One end of MFTF has been completed, along with its main magnet and some of its cryopanels. These systems were tested in February 1982. The actual pressures measured were compared with the predicted pressures from the simulation. Section 5 discusses the acceptance test and the quality of the predictions. Finally, Section 6 reviews the development of the MFTF vacuum system and draws conclusions from it.

2. MFTF VACUUM ENVIRONMENT

Magnetic Mirror Fusion machines form one of several approaches to magnetic fusion energy being pursued by the U.S. DOE, as well as researchers abroad. LLNL is the lead U.S. Laboratory for mirror machines. The current configuration of MFTF (designated MFTF-B (axicell)) consists of a solenoid with 12 circular magnets, two axisymmetric mirror cells at each end of the solenoid, then, on each end, two transition coils which reshape the plasma to map the solenoidal field lines to those of the large Ying-Yang magnets which act as plugs. Figure 1 shows a drawing of the vessel and the magnets. The machine itself is 58 m long. The solenoid part of the vessel is 8 m in diameter, and the end tanks are 10.6 m in diameter. Depending on the type of experiment being run, shots will last either .5 seconds or up to 30 seconds. Shots will be repeated as often as every five minutes. The expected ratio of power in to power out for MFTF equivalent D-T performance is .2 - .6 depending on mode [1].

The plasma is formed by energetic D_2 gas injected into the magnetic field by neutral beam injectors. In a typical neutral beam injector, 30 Torr liters/second enter the system, 3 Torr liters/second of which are properly aimed energetic neutrals. Of the energetics, less than 1/4 are usually trapped by the plasma. Therefore, 29+ Torr liter/second per injector end up as free gas which must be pumped in the system. There are 24 neutral beam injectors; 16 run for .5 seconds and the remainder run for 30 seconds.

The vacuum requirements for MFTF, set by the physics requirements, are stringent. The base pressure just before a shot must be less than 2×10^{-8} Torr, and during a shot as low as 6×10^{-8} Torr. Partial pressure of H_2 and He during a shot must be 3×10^{-9} Torr and partial pressure of HD 1×10^{-8} Torr. The gas loads on the system are essentially He, H_2, HD and D_2. The system will be well cleaned before sealing, and the large amount of LN_2 cooled surfaces about the vessel will trap ambient water and other high Z contaminents during operation. The sources of gas during a 30-second shot are:

D_2	7500 Torr liters from neutral beam injectors
He	4.5×10^{-3} Torr liters reaction product
	3.0×10^{-4} Torr liters cryogenic system leakage
	1.5×10^{-2} Torr liters contaminent in D_2
H_2	2.3×10^{-3} Torr liters reaction product
	3.0×10^{-3} Torr liters outgassing
HD	22.5 Torr liters contaminent in D_2.

Pumping is provided by a rough vacuum system, 10 external cryopumps, internal cryopanels and either titanium or vanadium getters. The rough vacuum system is conventional. The cryopumps have a pumping speed for D_2 of 250,000 liters/ second. Six of the cryopumps will be used only for initial pumpdown and periodic cryopanel regeneration. The other four will be subcooled and doped with argon in order to pump the He, H_2 and HD between shots. The entire external vacuum system will be valved off during an experimental shot. Figure 5 shows a schematic of the external vacuum system.

All of the pumping during the shot will be by the cryopanels and getters. Getters will be used as required in regions of high charge-exchange flux during shot startup, to prevent excessive release of absorbed surface gases. Alternatives to between shot gettering are being actively explored. Some of the plasma facing surfaces of the machine components are subject to moderate charge-exchange fluxes throughout the shot; it may be desirable to provide surfaces which can trap these particles. The plasma dumps in the end domes will be trapping surfaces. All particles absorbed by the plasma eventually make their way to the end dumps. The surface of the end dumps will be either vanadium or titanium and at least 80% of the incident particles will be buried. Almost no HD is pumped by the cryopanels. Instead the HD will eventually be absorbed by the plasma and transported to the end dumps where at least 80% will be trapped, leaving 4.5 Torr liters to be pumped by the cryopumps after a 30 second shot.

Most of the gas to be pumped is D_2, and most of the pumping will be on the cryopanels. There will be approximately 1200 M^2 of cryopanels in the vessel, located in the following places:

End zone arrays	275 M^2 each end
Neutral beam panels	225 M^2 each end
External beam and dump tanks	200 M^2 total

Figure 2 shows the placement of the cryopanels in the end tanks. Figure 1 shows the placement of the external beam tanks. Figure 3 shows a typical injector tank. These tanks are designed so that only 1% of the injected gas escapes into the main vessel as non-energetic particles. Thus, a typical injector tank with one injector will be a 3 amperes source of non-energetic gas.

The pressure must be low in the system for two reasons. Cold gas hitting the plasma will cool it down, killing the reaction, and the neutral beams lose power as the line density between them and the plasma increases. Different parts of the plasma can, however, tolerate different gas loads. The five regions of the machine -- Center cell, Axicell, Transition, Anchor and End -- are indicated in Fig. 1. The allowable apparent densities at the plasma for MFTF are given in Table 1. The allowable beam losses should be consistent with achieving the required energetic neutral flux to the plasma.

We say "apparent density" since what matters is the actual numbers of particles hitting the plasma. If the gas were uniform and isotropic, the apparent density next to the plasma would be the same as the actual density, but we do not assume an isotropic source. The cold gas which exits from the neutral beam tanks is likely to be very directed, and it is pointed straight at the plasma. The apparent density is the density which would produce the actual number of particles incident on the plasma.

The requisite densities are achieved by proper placement of the cryopanels and placing of baffles between zones. The plasma itself acts as a pump and in regions with no sources, the plasma may be used as a pump for the adjacent region. Thus the axicell region is baffled off from the transition region, but open to the center cell. The plasma in the center cell pumps the gas in the axicell, bringing both regions to permissible densities. The end zone is baffled off from the anchor zone. During a shot, the HD will move to the end zone, and stay there until the between shot external pumping.

3. EVOLUTION OF THE VACUUM SYSTEM

From The first proposal for MFTF to the present, the design has evolved from a single magnet verticle axis machine to the present multimagnet, horizontal axis, tandem mirror machine. The changes allow for more and better physics experiments. As the design changed, the vacuum requirements changed. As will be discussed below, the allowable density in the anchor region was lowered by a factor of 50.

The external vacuum system, which is not particularly affected by space limitations and uses standard technology, simply increased in size as the machine increased in size. For example, the number of external cryopumps went from 5 to 10. The cryopanels, on the other hand must fit inside the vessel, and they have been much affected by the changes.

It was decided when MFTF was first being designed to put as many cryopanels into the vessel as would reasonable fit. At that time, the gas loads and distributions were not perfectly understood. It was estimated that 1000 M^2 of cryopanels would suffice with a large safety margin (based on gas balance calculations). The problem was to settle upon the specific design of the panels and to decide how to place them in the vessel.

The liquid helium cooled surfaces of the cryopanels must be shielded from ambient radiation by optically opaque shielding by liquid nitrogen cooled surfaces. Several dozen different shielding designs were considered. In the winning design, the panels are made of "Z" shaped LN_2 cooled aluminum extrusions with the LHe cooled pieces between them. Figure 4 shows the "Z" configuration. The figure also shows more and less preferred directions of entry. Gas particles entering in the more preferred direction have a .56 probability of reaching the LHe panel and particles entering in the less preferred direction have a .12 probability. Thus, the parallel placement of "Z" configuration panels shown in figure 4, a natural first idea, necessarily presents on one side the less preferred direction to an entering gas particle. Further, particles can pass all the way through parallel panels without being captured by either side. 15% of the particles will indeed do so. If, however, the panels are tipped together to form an accordian pattern, as shown in figure 4, entering particles see preferred directions from both sides, there is no conductance through the array, and the capture fractions are higher.

The Monte Carlo code described in the next section was used to estimate capture fractions for the various designs. It estimated that 30% of the particles entering a single "Z" from an isotropic source would reach the LHe panel and be absorbed. (In estimates of operating density, we assumed that

25% would be captured in order to provide a conservative estimate and to allow for manufacturing tolerances.) The code further estimated that 40% of the particles entering a parallel array would be trapped but 65% of the gas entering a V of the accordian array would be trapped. In all, the first designs called for 28 separate panels in the vessel. If the same design was used for the tandem design, 36 panels would be required. In the event, only 28 of the original panels will be used.

The panels were removed generally to make room for other systems. The Ying Yang magnets are larger than in the first design and the plasma is larger. Further, in the end zones, the panels must be shielded from the 20% of energetic particles not trapped in the dumps. If an energetic particle hits a cryopanel before it thermalizes, as many as 100 water molecules may be dislodged. These shields take up more of the space originally allotted to the cryopanels. As a result, the accordions now contain three rather than four panels each.

Meanwhile, the vacuum requirements became more stringent. In the anchor region, for example, the allowable density was 1×10^{11} particles per cc in the first design. It is 2×10^{9} particles per cc in the current design. This combination of fewer panels and stricter requirements necessitated reducing the amount of gas from the neutral beam injectors. The number of injectors needed has been reduced from about 40 to 3 in each end tank, and the injectors themselves are placed in tanks with pumping. 200 M^2 of cryopanels are placed in the neutral beam injector and dump tanks. Still, the stricter requirements and the fewer cryopanels have been paid for in part with safety margin. The early designs had densities estimated at 50% or less af allowable, while the current design finds estimated densities as much as 75% of allowable.

4. METHODS OF ANALYSIS

The efficiency and effectiveness of an arrangement of cryopanels must somehow be estimated. Stringent requirements are set by the physicists. The sources of gas are well understood, but the transport of gas from the source to either the plasma or the cryopanels is complicated, and different placements of cryopanels can result in significant differences in the final distribution of the gas.

A standard gas balance was calculated for the MFTF fusion chamber as a first approximation to the equilibrium conditions. The chamber is broken into zones. The sources, sinks and connections between the zones, worked out from the geometry of the system, are input, and the equilibrium pressure in each zone is calculated by standard techniques. While this method provides reasonable estimates, it depends on the assumption that the gas in the system is Maxwellian. That assumption is not fulfilled. The sources of gas are the neutral beam injectors and dumps and the plasma dumps, localized sources not uniformly placed about the chamber. The gas from the neutral beam injectors leaves the neutralizer duct more directed along the axis of the neutralizer than a simple cosine distribution. For example, in a 6 x 6 x 20 duct, particles entering with the cosine distribution leave according to an approximate cosine^2 distribution. These neutralizers are pointed directly at the plasma, and so more gas will reach the plasma than the standard Maxwellian theory would call for, making the apparent density at the plasma higher. Also, the zones in the gas balance equation are very large. Conductance between the zones is difficult to estimate, and sometimes estimates of differing pressures within the zones are necessary. Finally, the effect of baffles and shields are very difficult to estimate using a standard gas balance. The end zone cryopanels are shielded from the plasma dumps so that no particle can go directly from the dump to the cryopanels, but the effects of these shields cannot easily be modeled in a gas balance code.

A three-dimensional Monte Carlo code has been developed at LLNL to allow for more detailed study of the vacuum system. The first version was written in 1978, and it has been improved over the years as the analysis has become more complex. In its present form it can:

1. Determine where particles from a source are absorbed,
2. Determine the distribution of lifetimes of a particle from a source,
3. Estimate equilibrium densities at points in the chamber,
4. Estimate line densities,
5. Estimate rise times.

The geometry of the vessel is modeled in fairly fine detail. All the cryopanels, magnets, baffles, walls and domes are included. Supports are generally left out. The geometry is modeled with flat plates fitted together, so the cylandrical wall becomes an 8-sided (or, occasionally 16-sided) regular polygon. The plasma is modeled with triangles, and the magnet with quadrilaterals. The cryopanels are retangular boxes. Every surface has a sticking coefficient and a temperature.

The Monte Carlo methods used are standard.[2] Complex variance reduction techniques are not used since straight simulation will produce statistically adequate results in reasonable running times. (LLNL has large, fast computers). Particles are generated at the source with a distribution chosen according to the specified initial distribution (usually the cosine distribution). An initial temperature is also specified. The particle moves through the system in a straight line until it hits the next surface. If the surface has a sticking coefficient greater than 0, a random number decides whether the particle is absorbed by the surface. If not, a new direction is chosen, drawing from the cosine distribution centered about the normal to the surface. The particle is assigned the temperature of the surface, and proceeds on its path.

A density at a point is estimated as follows. A sphere is defined about the point, with radius 60 cm in typical MFTF chamber problems. As the particle moves, the amount of time spent in the sphere is calculated. Finally, the average amount of time spent in the sphere by a particle entering from the source is calculated from the individual particle histories. Each particle always has a temperature associated with it. Its speed is taken to be the mean speed corresponding to that temperature. The time spent in the sphere is the distance traveled through the sphere divided by the speed. At equilibrium, the number of particles in the sphere is the number of particles entering at the source in the time an average particle spends in the sphere. Thus, if 1 x 10^{16} particles enters at the source per second, and each particle spends, on average, 1 millisecond in the sphere, then, at equilibrium, there will be 1 x 10^{13} particles in the sphere. The density at the point is the volume of the sphere divided into the number of particles. Line densities are estimated in a similar fashion, using cylinders about the line.

There are various sources of error in this method. The main ones include:

1. Statistical variation. Any Monte Carlo estimate is subject to sampling errors. An estimate of this error is made concurrently with the Monte Carlo estimate.

2. Geometry errors. Even though it is detailed, there are necessary simplifications in the the geometry.

3. Physics assumptions. The simulation of particle transport uses assumptions about particle behavior, such as directions following the cosine

distribution or the independence of incident and reflection angles when a particle hits the surface, which are generally agreed to in the literature and attested by experiment. However, errors and imperfections in the theory may cause errors in the simulation.

4. Physics simplifications. The program makes several simplifying assumptions. Intermolecular collisions are ignored. One speed associated with a given temperature, rather than a speed distribution. A particle hitting a surface comes off with a fixed temperature, a function of particle input temperature, surface temperature and accomodation coefficient, rather than a random temperature.

The magnitude of the last three errors is difficult to determine. However, experience with Monte Carlo methods and comparison of simulated results with well-known values made us very confident that the statistical errors controlled by sample size to about 10%, was larger than the total error from other causes. In the next section, we describe the comparison of simulated results with experimental results.

The Monte Carlo code has been used on three levels of complexity. The individual pieces of the cryopanel arrays were extensively analysed. The "Z" design was compared to over 40 other different possible designs. Heat loading and x-ray absorption by the designs was analyzed along with trapping fractions. Then, the characteristics of differing arrangements of panels was studied. A result of this analysis, comparing parallel panels with the adopted accordian design was mentioned above. Finally, the entire chamber was modeled. Point and line densities were estimated throughout the machine. The fraction of particles from various sources actually hitting the plasma was determined, and the relevant apparent densities computed. The relative effectiveness of different cryopanels was also considered, and when space was needed, less effective panels were removed. It is these analyses which provide most of the estimates in the earlier sections of this paper. Our Monte Carlo code has proved a valuable, versatile and powerful tool for predicting the performance of the internal vacuum system and showing that the design would meet the physics and experimental requirements.

5. The Technology Demonstration Test

One of the end vessels of MFTF has been completed. (This vessel was to have been the original experimental vessel.) In February, 1982, the vessel, with the Ying-Yang magnet and six of the eight neutral beam cryopanels installed was sealed and the various components were tested. On February 24, the cryopanel pumping was tested. The external vacuum system was valved off. D_2 gas was injected through each of three nozzles sequentially at a rate as 440 Torr liters/second. Five ion gauges placed about the vessel recorded the increase in pressure. The flow was maintained until the gauge readings stabilized (typically, 25 seconds). Injection at each nozzle was repeated several times. The stabilized readings showed great consistency, with only one gauge-nozzle combination showing a variation of more than 5%.

Meanwhile, our three-dimensional Monte Carlo code was used to estimate the gauge readings with various combinations of the cryopanels working. Estimates were provided for the case when all the cryopanels were working, and all believable cases where one or two cryopanels had failed. Since two pairs of cryopanels were plumbed in series, not all combinations of one and two cryopanels off were possible.

Errors in the simulation might arise from the following factors.

1. Statistical variation. The simulation had an empirically estimated relative standard deviation of 10%.

2. Parameter estimates. The main surface of the cryopanels were assumed to trap 25% of the incident particles, and the pumping edges 18% of the incident particles. The estimated densities depended upon these values. The average density is 15% lower if the main face captures 30%.

3. The simplified geometry. The vessel, the magnet and the cryopanels were modeled, but the framing and supports were not. The path from one nozzle to one of the gauges is unobstructed, but the path away from the gauge is constricted by one of the magnet seismic supports. And, that gauge read significantly higher than all the other gauges when that nozzle was turned on.

The average pressure (that is, the average of the 15 measurements) was 25% lower than predicted by the simulation. The recorded pressures were compared with the 13 possible scenarios of one or two panels off or all working. The comparison looked at the sum of the absolute value of the differences between the predicted and the actual readings. It was found that the scenario closest to the actual readings was where all the cryopanels worked. Other evidence also pointed to all the cryopanels working, and that was the conclusion of the test. The predicted and recorded pressures for one nozzle injection are shown in Table 2.

Thus, the Monte Carlo estimates were too high, by about 30%. It is likely that the pumping speed of the panels is higher than the 25% trapping fraction assumed. But there may be other factors, including bias in the gauges. However, the simulation estimates clearly provided a reasonable and conservative estimate of cryopanel performance, and this fact gives us confidence in the prediction of operating pressures made in the earlier sections.

6. CONCLUSIONS

At the time of writing, the design for MFTF was not final. The internal vacuum system has survived several machine design changes. It is smaller but not significantly changed from the first worked out design. The original design principle was to fill the vessel with as many cryopanels as reasonable, but have the cryopanels of uniform design and rectangular shape to allow for relative ease of manufacture.

The use of the three-dimensional Monte Carlo code has been very valuable in the design of the vacuum system. It has been used throughout the design process, and is still contributing. The acceptance test showed that the Monte Carlo estimates provide reasonable, conservative estimates of densities. Similar techniques should be useful in any large system extensively using cryopanels.

REFERENCES

1. A complete description of the Physics and Engineering status of MFTF-B (axicell) is in D. Baldwin and B. Logan, Physics Basis for an Axicell Design for End Plugs of MFTF-B, LLNL Report UCID-19359, 1982 and K. Thomassen and V. Karpenko, An Axicell Design for End Plugs of MFTF-B, LLNL Report UCID-19318, 1982.

2. The Monte Carlo Method is discussed in Hammersley and Handscomb, Monte Carlo Methods, Methuen and Co., London, 1965. Seminal work in applying Monte Carlo Methods to vacuum analysis was done by D. H. Davis of LLNL, and is reported in D. H. Davis "Monte Carlo Calculation of Molecular Flow Rates Through a Cylindrical Elbow and Pipes of Other Shapes," Journal of Applied Physics, V. 31, P. 1169, 1960.

FIGURES

Figure 1. Drawing of MFTF showing the beam tanks and magnets with the different zones indicated.

Figure 2. Drawing of one end of MFTF showing the location of the cryopanels.

Figure 3. Drawing of a neutral beam injector tank and the beam dump tank.

Figure 4. Drawing of a cryopanel "Z" extension, showing more and less preferred directions of entry, and the parallel and accordion arrangements of panels.

Figure 5. Schematic of the external vacuum system.

TABLE 1. Vacuum requirements and estimated apparent operating densities for MFTF.

Region	Requirement	Apparent operating density*
End	5×10^{10}	3.5×10^{10}
Anchor	2×10^{9}	1.2×10^{9}
Transition	2×10^{9}	**
Axicell	2×10^{10}	1.5×10^{10}
Center cell	2×10^{10}	1.5×10^{10}

*The apparent density is the density which would produce the same estimated number of particles incident on the plasma if the system were Maxwellian. See Section 2.

**Not presently determined.

TABLE 2. Predicted and recorded pressures for the technology acceptance test. Units are 10^{-5} Torr. Values are for top nozzle injection.

Cryopanels off	1	2	3	4	5	Average
None	4.0	3.0	4.3	2.9	3.4	3.5
B	4.3	3.5	5.5	2.9	3.7	4.0
C	4.8	4.3	7.3	3.2	4.2	4.7
D	4.9	3.6	6.8	4.8	4.2	4.9
E	4.4	3.2	5.2	4.3	3.8	4.2
B,C	6.1	5.2	7.9	5.1	5.5	6.0
B,D	6.4	4.6	6.5	5.4	5.5	5.8
B,E	5.1	3.8	6.7	5.9	5.1	5.3
C,D	6.9	6.2	9.4	6.0	6.3	7.0
C,E	5.2	5.2	8.2	5.5	5.8	6.0
D,E	5.7	5.5	7.1	7.3	6.6	6.5
A,B	5.5	6.0	6.8	4.7	4.5	5.5
E,F	5.2	4.9	6.5	6.2	5.1	5.6
Test results	2.4	2.6	3.2	2.7	2.5	2.7

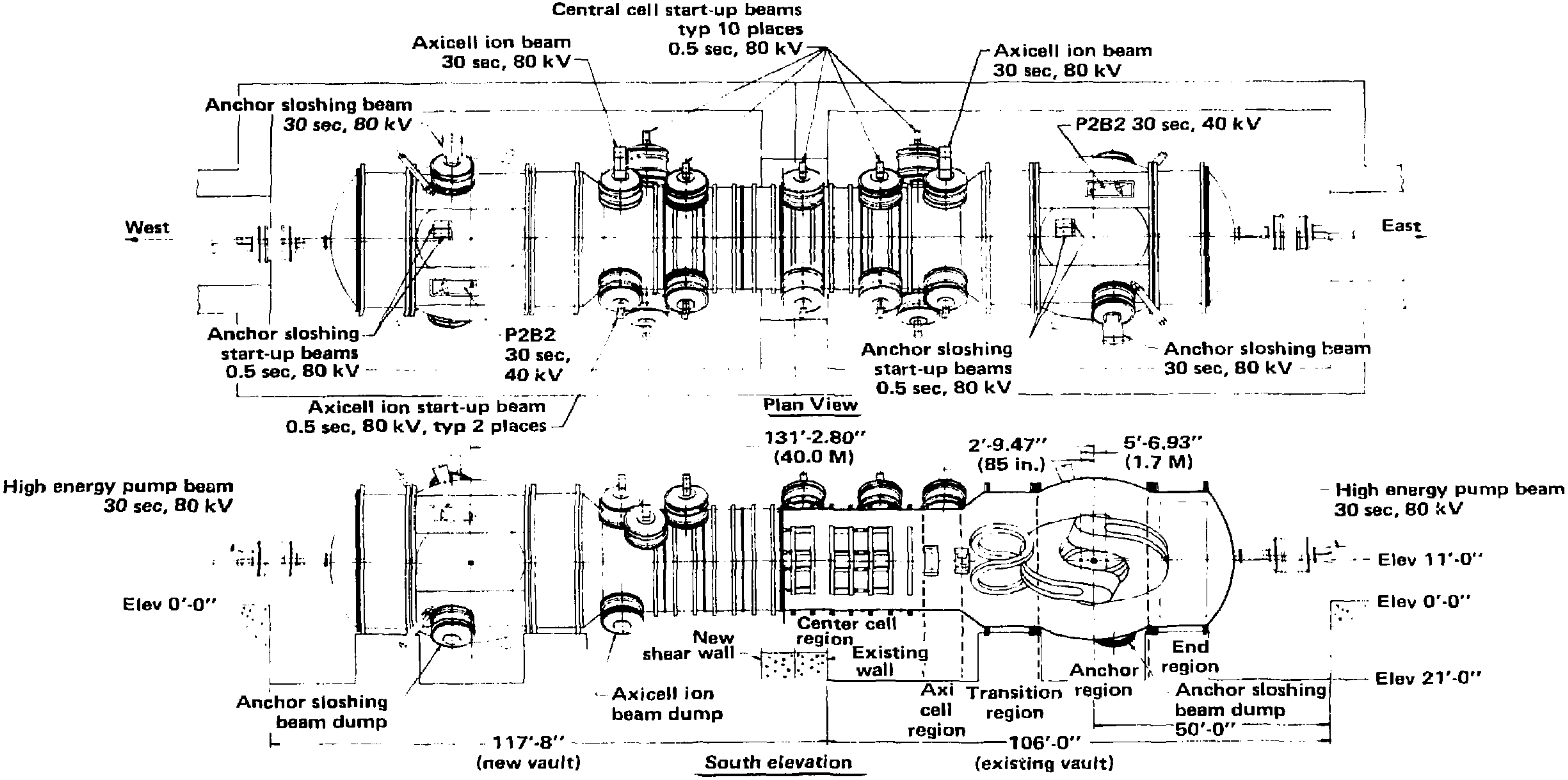
Central cell start-up beams
typ 10 places
0.5 sec, 80 kV
Axicell ion beam
30 sec, 80 kV
Axicell ion beam
30 sec, 80 kV
Anchor sloshing beam
30 sec, 80 kV
P2B2 30 sec, 40 kV
West
East
Anchor sloshing
start-up beams
0.5 sec, 80 kV
P2B2
30 sec,
40 kV
Anchor sloshing
start-up beams
0.5 sec, 80 kV
Anchor sloshing beam
30 sec, 80 kV
Axicell ion start-up beam
0.5 sec, 80 kV, typ 2 places
Plan View
131'-2.80"
(40.0 M)
2'-9.47"
(85 in.)
5'-6.93"
(1.7 M)
High energy pump beam
30 sec, 80 kV
High energy pump beam
30 sec, 80 kV
Elev 11'-0"
Elev 0'-0"
Elev 0'-0"
Center cell
region
New
shear wall
Existing
wall
End
region
Anchor
region
Elev 21'-0"
Anchor sloshing
beam dump
Axicell ion
beam dump
Axi
cell
region
Transition
region
Anchor sloshing
beam dump
50'-0"
117'-8"
(new vault)
South elevation
106'-0"
(existing vault)

Figure 1

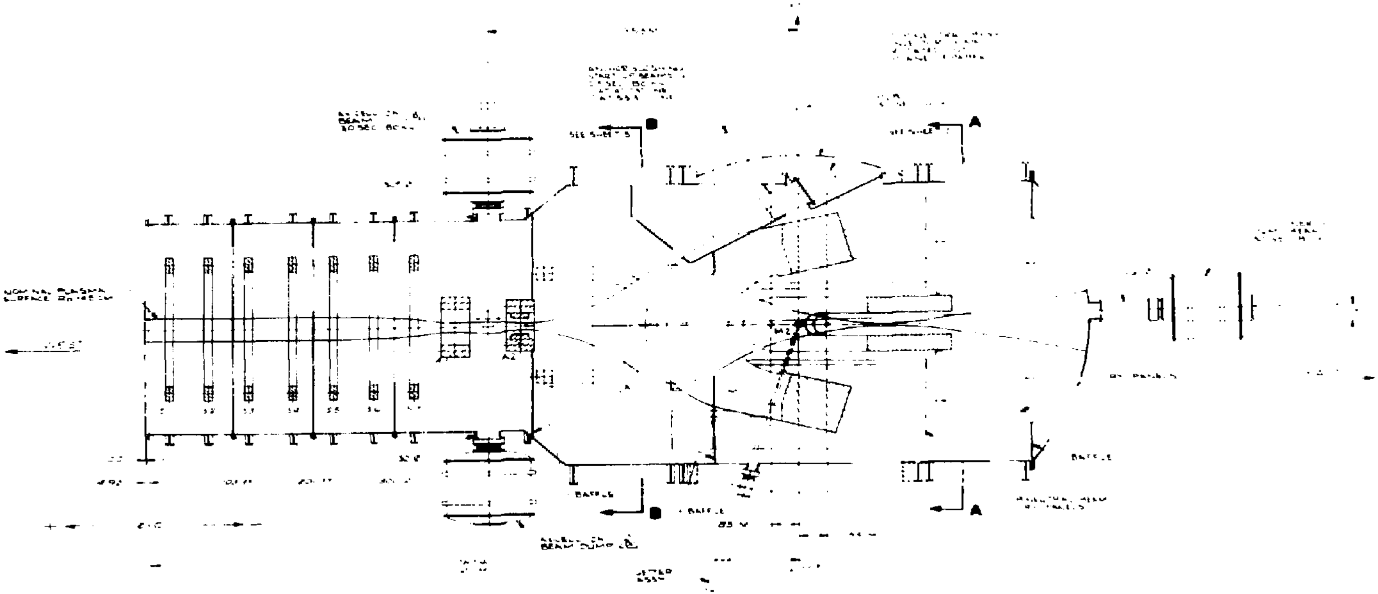
NOMINAL PLASMA SURFACE
SEE SHEET 5
A
A2
M2
BAFFLE
BAFFLE
BAFFLE
BEAM DUMP
GETTER ASSY

Figure 2

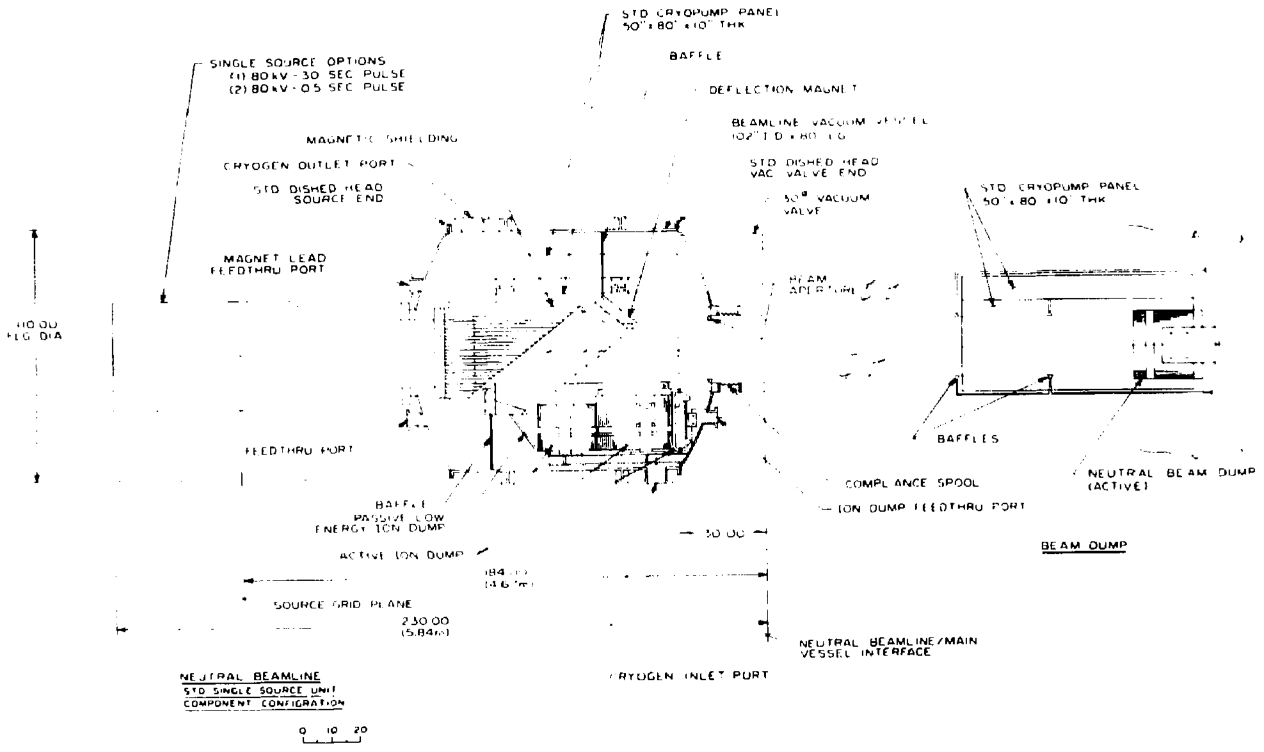STD CRYOPUMP PANEL 50" x 80" x 10" THK
BAFFLE
DEFLECTION MAGNET
SINGLE SOURCE OPTIONS
(1) 80 kV - 30 SEC PULSE
(2) 80 kV - 0.5 SEC PULSE
MAGNETIC SHIELDING
CRYOGEN OUTLET PORT
STD DISHED HEAD SOURCE END
BEAMLINE VACUUM VESSEL 102" I.D. x 80" LG
STD DISHED HEAD VAC VALVE END
30" VACUUM VALVE
STD CRYOPUMP PANEL 50" x 80" x 10" THK
110.00 FLG DIA
MAGNET LEAD FEEDTHRU PORT
BEAM APERTURE
FEEDTHRU PORT
BAFFLES
COMPLIANCE SPOOL
NEUTRAL BEAM DUMP (ACTIVE)
BAFFLE
PASSIVE LOW ENERGY ION DUMP
ION DUMP FEEDTHRU PORT
30.00
ACTIVE ION DUMP
BEAM DUMP
184.00 (4.67m)
SOURCE GRID PLANE
230.00 (5.84m)
NEUTRAL BEAMLINE/MAIN VESSEL INTERFACE
CRYOGEN INLET PORT
NEUTRAL BEAMLINE
STD SINGLE SOURCE UNIT
COMPONENT CONFIGRATION
0 10 20

Figure 3

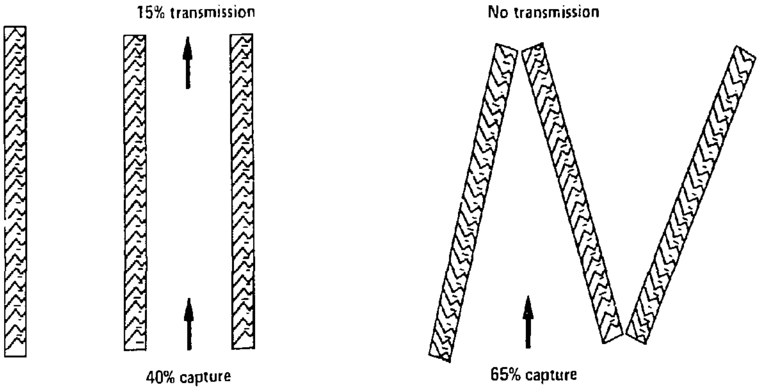

Parallel array

Accordian array

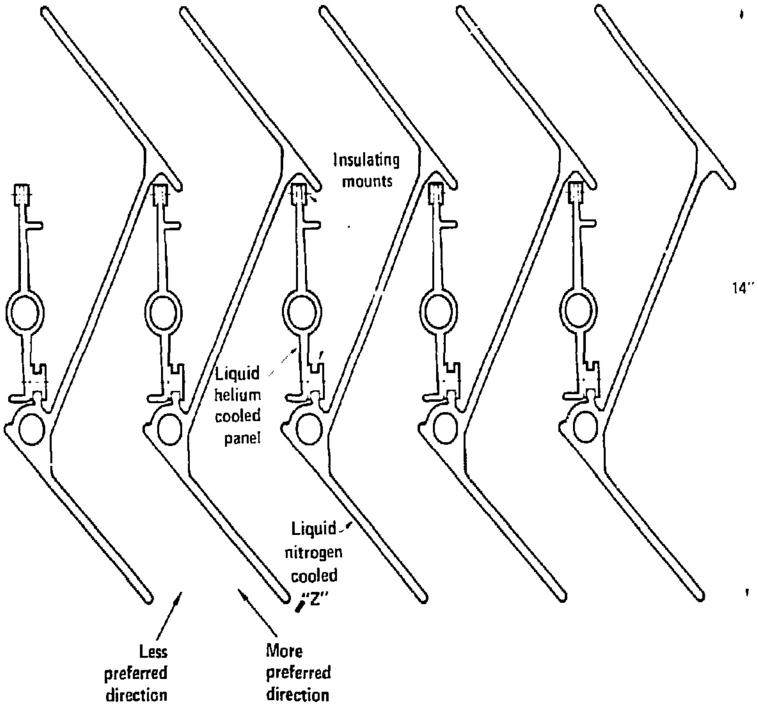

Figure 4

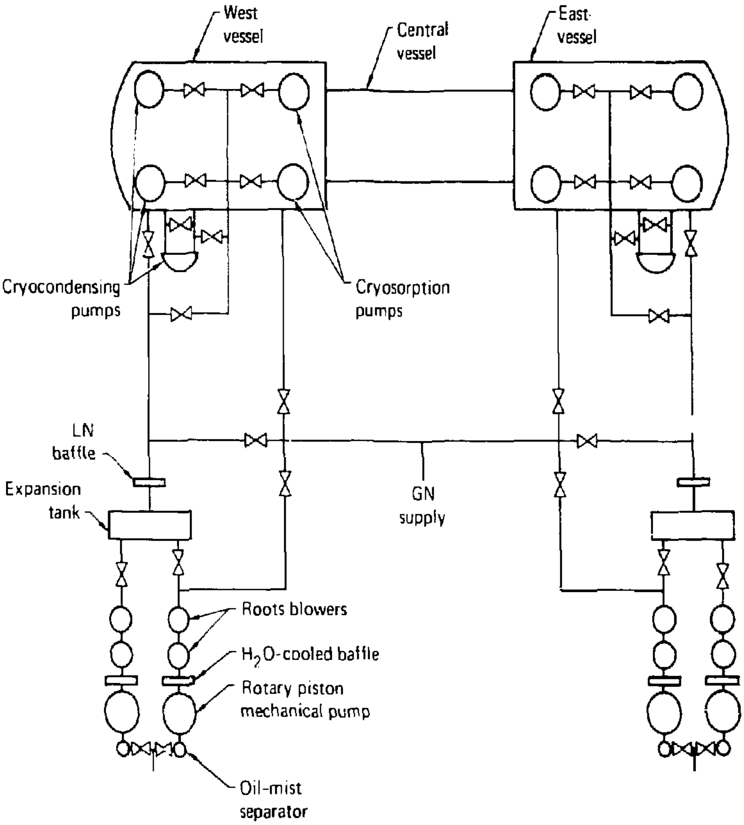
West vessel
Central vessel
East vessel
Cryocondensing pumps
Cryosorption pumps
LN baffle
Expansion tank
GN supply
Roots blowers
H2O-cooled baffle
Rotary piston mechanical pump
Oil-mist separator

Figure 5